PHYSICAL REVIEW B **78**, 161405(R) (2008)

Modeling realistic tip structures: Scanning tunneling microscopy of NO adsorption on Rh(111)

J. H. A. Hagelaar and C. F. J. Flipse*
Department of Applied Physics, Eindhoven University of Technology, P.O. Box 513, 5600 MB Eindhoven, The Netherlands

J. I. Cerdá
Instituto de Ciencia de Materiales de Madrid, ICMM-CSIC, Cantoblanco, 28049 Madrid, Spain
(Received 15 September 2008; published 27 October 2008)

We have performed a joint experimental and theoretical scanning tunneling microscopy (STM) study of NO adsorbed on Rh(111). The experimental STM images showed a strong sensitivity to the tip conditions that could be altered by dipping the tip into the sample or by application of voltage pulses. Only via STM simulations performed over an exhaustive range of tip-apex terminations, including several contaminants in different adsorption geometries and with different spatial orientations, we have been able to reproduce the rich variety of measured images. From the analysis, we are able to infer a realistic structural model for the ultimate tip-apex structure involving apex geometries considerably more complex than those typically employed in STM modeling.

DOI: 10.1103/PhysRevB.78.161405 PACS number(s): 68.37.Ef, 68.35.B−

At present, the theoretical simulation of scanning tunneling microscope (STM) images[1] may be regarded as a mature field. A wide range of formalisms going beyond the seminal work of Tersoff and Hamann[2] have been developed during the last two decades, mainly focusing on the relevant role played by the tip in the final aspect of the image.[1,3–7] Despite the formalisms differing in the way the entire STM setup is modeled at the atomic level or the level of accuracy used to calculate the electronic Hamiltonian, a reasonably good level of agreement is routinely achieved between theory and experiment.

It is well established that the influence of the tip is greatest when a foreign species (atom or molecule) is adsorbed on the tip apex: a so-called functionalized or contaminated tip.[8,9] Such apex terminations may enhance or modify the image aspect or even provide chemical contrast.[10–13] Indeed, it is often the case that experimental images lacking the expected symmetry or not presenting well resolved atomiclike features are either discarded by the experimentalist or cannot be reproduced by the theorist, presumably because the precise apex chemical identity and/or orientation are well off simplified tip models typically employed in the simulations. Paradoxically, such images offer a wealth of information about the tip-apex structure, which is still the main unknown in the STM experience.

In order to extract such information, one may adopt an opposite view to what is generally followed in STM imaging, i.e., use the surface adsorbates to probe the tip-apex structure. Here, we demonstrate how a well characterized surface system, namely, NO on Rh(111), can be used to extract the nature and relative orientation of the most relevant tip orbitals involved in the surface imaging. To this end, we have acquired a rich variety of experimental images for this system after tip manipulation experiments which were later compared against theoretical simulations comprising a wide range of tip configurations. Despite that each type of experimental image can be well reproduced by several different apex geometries, a unified picture for the ultimate tip structure compatible with our tip manipulation procedure may only be achieved if blunt metallic tips exposing a large variety of adsorption sites are assumed. It should be recalled that, currently, there hardly exist any alternative techniques which can provide such a detailed insight into the tip-apex structure.[14–16]

NO adsorption on Rh(111) is a system of catalytical interest:[17] the ability of Rh to efficiently dissociate NO makes it the most suitable metal for the removal of nitric oxide in automotive exhaust systems. In UHV, NO is known to adsorb molecularly on Rh(111) below $T \sim 250$ K presenting a complex phase diagram which comprises several ordered structures.[18–20] In this study, we will concentrate on the hexagonal $p(2\times 2)+2$NO and the rectangular $(2\times\sqrt{3})+2$NO phases—both depicted in Fig. 1: they consist of zigzag chains of alternating NO species adsorbed at hcp and fcc sites. The relative orientation of each chain with respect to its neighbor chain, separated by a $\sqrt{3}a$ distance, distinguishes one phase from the other. In all cases, the NOs are adsorbed upright with the nitrogen atom closest to the metal.

A clean Rh(111) single crystal was mounted on a sample plate and cleaned by repeated cycles of Ar^+ sputtering at 500 °C (1.5 μA for 90 min), and annealing at 500, 600, and 700 °C for 20 min for each temperature. The sample was then flashed to 1200 °C. The electrochemically etched tips were made from polycrystalline tungsten wire using standard etching techniques. In order to remove the WNO_3 layer that forms in air, the tips are heated up to temperatures >1200 °C, above which the WNO_3 sublimes and a clean tungsten tip results.[21,22] After cleaning, both tip and sample

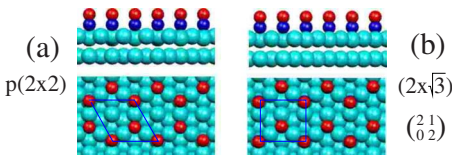

FIG. 1. (Color online) Top and side views of the two Rh(111) +2NO phases considered in this work: (a) $p(2\times 2)$ and (b) $(2\times\sqrt{3})$. The precise matrix notation for the supercell in (b) is also given. Red/gray, blue/dark gray, and light blue/light gray atoms represent the O, N, and Rh, respectively.

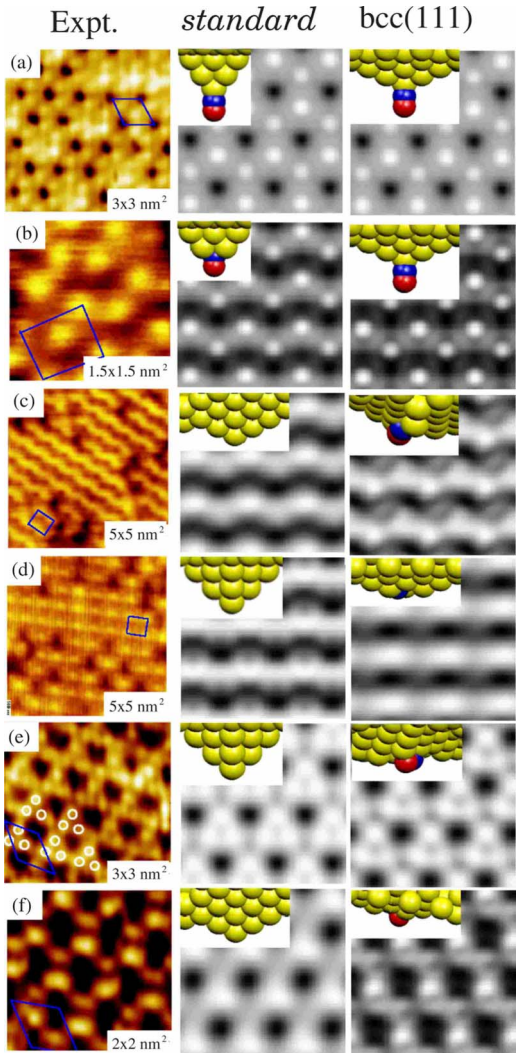

FIG. 2. (Color online) Left column: experimental STM images acquired for the (2×2) and $(2\times\sqrt{3})$ phases under tunneling conditions: $V=-0.1$ V and $I=0.2-0.4$ nA. The unit cell in each case is indicated by the blue/dark gray lines while the size of each image is also indicated at the bottom. Middle column: theoretical simulations that best match the experimental ones using *standard* tips. The inset shows the type of tip employed and its orientation relative to the surface normal. Red/gray, blue/dark gray, and yellow/light gray atoms represent the O, N, and W, respectively. Right column: same as middle column but employing bcc(111) oriented tips. Size for all theoretical images is (0.8×0.8) nm^2. See text for further explanations.

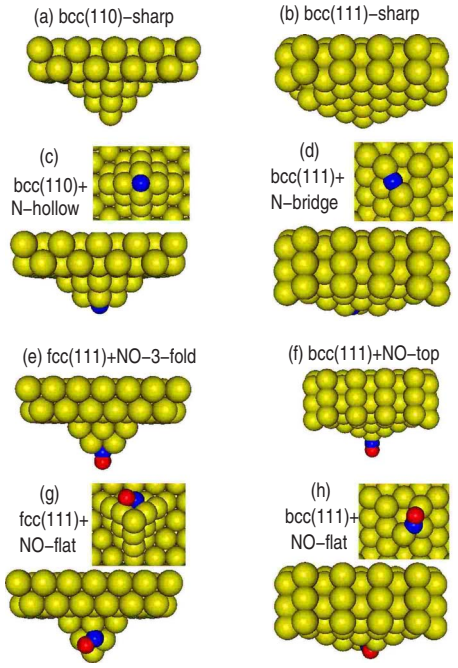

FIG. 3. (Color online) Side views of the DFT optimized geometries for different tip termination models. (a)–(c) and (e), (f) correspond to symmetric *standard* configurations while the rest involve N or NO adsorption at nonsymmetric sites. Bottom views revealing the NO or N adsorption site are also displayed for tips (c), (d), (g), and (h).

are mounted in the Omicron GmbH LT-STM. The NO adlayer is then formed by exposing the clean Rh(111) substrate at 200 K to NO gas. Being present during this procedure, the tip will also be contaminated by molecules.

In the left column of Fig. 2 several different experimental appearances of the $p(2\times2)$ and $(2\times\sqrt{3})$ phases are shown. All images were acquired under the same tunneling conditions: $I=0.2-0.4$ nA and $V=-100$ mV. Changes between the different types of imaging could be induced either by dipping the tip into the substrate or by applying voltage pulses of ±10 V. Remarkably, the images show a strong sensitivity to the tip conditions and, hence, they may be regarded as valid probes for *imaging* the tip apex. Figures 2(a) and 2(b) correspond to the $p(2\times2)$ and $(2\times\sqrt{3})$ phases, respectively, showing well resolved bumps and hardly any contrast difference between fcc and hcp NO sites. The most frequent aspect of the $(2\times\sqrt{3})$ phase is in the form of wiggly stripes such as those displayed in Figs. 2(c) and 2(d). The image in Fig. 2(e) shows a $p(2\times2)$ arrangement but is completely different from what might have been expected based on the positions of the molecules (see Fig. 1). Bright dots form an equilateral triangle, highlighted with white circles in the figure. Although the image might easily be misinterpreted as a more densely packed 0.75 ML $(2\times2)+3$NO phase, we will show below that this is not the case. Finally, Fig. 2(f) corresponds to an image of the $p(2\times2)$ phase presenting a clear contrast between the two NOs in the unit cell, although we cannot infer from the image the identity of each bump.

It is clear that, however, information on the tip structure cannot be extracted directly from the visual analysis of the images as indirect techniques are required instead. We have tackled this problem by performing STM simulations for both phases employing a large variety of plausible tip models. Our tip modeling follows the approach described in Ref. 5. We considered a semi-infinite W-bcc surface oriented both along the (111) and (110) directions as well as a hypothetical W-fcc phase (111) oriented. As depicted in Fig. 3, below the surface we stacked an isolated pyramid (the apex) comprising several tens of atoms. Sharp tips were modeled by one atom terminated pyramids while blunt tips were obtained after removing the end atom. Apart from these clean tips, we also considered several contaminant species (N, O, and NO)

adsorbed in a variety of sites: for sharp tips we placed the NO either below the end atom (on top site) or at the side of the pyramid. For blunt tips we positioned the contaminants at the most symmetric exposed site. The trial geometries were optimized via density-functional theory (DFT) based calculations employing the pseudopotential linear combination of atomic orbitals (LCAO) SIESTA code[23] under the generalized gradient approximation (GGA).[24] In the *ab initio* calculations we replaced the semi-infinite surface by tungsten two-dimensional (2D) slabs of different thicknesses depending on the crystal orientation. The apex atoms were placed in a $p(4\times4)$ supercell in order to minimize apex–apex interactions and were fully relaxed while leaving the slab atoms fixed to the bulk positions. Some representative cases are displayed in Fig. 3. We note that bcc(111) tips present large in-plane atomic distances and a reduced interlayer separation, thus leading to much more blunt tips than the rest. For such blunt tips, we found that adsorbates initially placed at the threefold site induce a large reconstruction of the surrounding W atoms since the N atoms tend to adopt a pseudo-bridge configuration [see Figs. 3(d) and 3(h)]: in the latter case, for instance, the NO ends up in a slightly planar geometry.

The theoretical STM images were all calculated employing the GREEN code[4] under the extended Hückel theory (EHT) approximation.[25] The formalism represents a fast yet reliable scheme for obtaining topographic images which can be directly compared against the experimental ones. Specific EHT parameters were associated to each tip and surface phase after accurately fitting the density of states projected on the atoms to their *ab initio* counterparts. Since in the STM simulations the apex is described as nonperiodic,[4] we may also consider tilted tip geometries whereby the entire tip-apex block is rotated with respect to the surface normal. We studied both azimuthal and polar rotations thus introducing two further degrees of freedom for each tip termination.

The center column in Fig. 2 presents a set of simulated images calculated employing *standard* tip-apex models (see the insets in each image). By *standard* we refer to symmetric structures with the bulk tip normal plane aligned with that of the surface. To the right of each experimental image, we display the one providing a best fit to its experimental counterpart. In most cases, apart from a satisfactory visual agreement, a close correspondence is also obtained between the measured and calculated overall corrugations, d, in the topographic maps; d varies between 0.2–0.4 Å in all images except for Fig. 2(a), where d=0.6 Å. Also note the modest agreement reached for Fig. 2(f) since, although the simulation with a clean bcc(111) tip shows a slight contrast between the fcc and hcp sites, the bumps are not well resolved. Most importantly, we obtain marked differences in the nature and structure between the tips assigned to each type of image, proving that the system is particularly suited for extracting information on the tip-apex structures.

We next address the sensitivity of the simulations to the precise tip structure and orientation. Although tip manipulation experiments have shown that the apex structure may suffer strong changes,[16] it is not likely that, as the outcome of each tip manipulation, one will encounter the *standard* tips displayed in the central column of Fig. 2. For instance, how can a transition from a bcc(111) orientation to a (111) take place at the apex by simply dipping the tip into the adsorbate layer? We have therefore searched for alternative, less *standard* tip terminations which could explain more naturally the occurrence of such a diversity of experimental images. Indeed, we have found that most types of images could be reproduced with different tip models after applying appropriate rotations to each tip. We present in the right column of Fig. 2 a set of images, all of them simulated assuming a bcc(111) tip orientation with NO or N species adsorbed at different sites. The general agreement is even better than that obtained with the *standard* tips. Notice that, for instance, Fig. 2(f) is now satisfactorily reproduced.

Let us first focus on the highly resolved images of Figs. 2(a) and 2(b). Our calculations reveal that such images are well reproduced with tips ending with a NO species standing upright, irrespective of the positions of the W atoms above it, e.g., models (e) or (f) in Fig. 3. This result is robust against both azimuthal rotations and small tilting of the tip. Decomposition of the tunneling current into different paths shows that the main contributions arise from the π^*_{xy} molecular orbitals (MOs) of the NOs both at the tip and on the sample. Despite that these MOs show up as bright rings in local density of states (LDOS) maps, placing the tip NO on top of a surface NO maximizes the interactions between their π^*_{xy} states, thus yielding well resolved bumps.

The stripes associated to the $(2\times\sqrt{3})$ phase [Figs. 2(c) and 2(d)] are already nicely reproduced with *standard* clean tips [Figs. 3(a) and 3(b), respectively], indicating that the W apex states are the active ones in the images. After tilting the bcc(111)+NO-flat tip in order to bring a W atom closer to the surface, the simulations (right column in the figure) also provide wiggly stripes as in Fig. 2(c). The additional dimmer features decorating the stripes are due to the tunneling via the apex NO states. In this case, rotations of the tip azimuth changed the aspect of the simulated images. On the other hand, the bcc(111)+N-bridge tip [Fig. 3(d)] reproduces remarkably well the stripes of Fig. 2(d). In this tip the N atom is essentially buried in between the W atoms so that most of the current comes from the three metal atoms, all with approximately the same intensity. Hence, we may conclude that striped $(2\times\sqrt{3})$ patterns are imaged by W apex atoms.

The three lobe structure surrounding each NO species in the counterintuitive image of Fig. 2(e) shows up in the simulations for the $p(2\times2)$ phase employing either a clean bcc(110) tip or the bcc(111)+NO-flat tip after a small tilt, bringing a W apex closer to the surface. Therefore, this type of image is again characteristic of W terminated tips. On top of a molecule, the main contribution comes from the σ_z and π^*_{xy} MOs interacting with the W p_z, d, and s states but there is a strong destructive interference between pathways involving the molecule's σ^*_s state which is responsible for the small depression on top of the NOs.

Fitting the experimental image of Fig. 2(f) is nontrivial since the inequivalence between the two bumps does not arise from any electronic structure differences between the two surface NOs; their respective LDOS are very similar. The theoretical image at the right column reproduces nicely this inequivalence; we employed the bcc(111)+NO-flat tip tilted so that both the NO molecule and an apex W atom are

exposed to the vacuum. A 45° azimuth rotation was additionally required. The large bump is associated to the fcc NO when it is placed midway between the apex O and W atoms. In this configuration, the π^*_{xy} states and, to a lesser extent, the σ_z yield the largest contributions to the current, mainly tunneling into/from the tip O-p_z and the W states. The smaller bump, associated to the hcp NO, shows up when the tip oxygen atom is close to it; now the π^*_{xy} contribution is greatly diminished and the σ_z becomes the dominant one.

One may cast the results for all the bcc(111) contaminated tips (right column in Fig. 2) into a unified realistic structural model for the tip apex. Our results are fully consistent with a blunt tip termination not necessarily bcc(111) oriented or well ordered, e.g., a droplet,[16] exposing a variety of adsorption sites to the NOs. Each tip dipping and retracting process will desorb/adsorb NO species from/at different sites. At the same time, large voltage pulses may cause NO dissociation, thus leaving individual N or O species at the apex. Furthermore, any of the two mechanisms may as well induce diffusion of the W atoms along the tip, generating different adsorption sites with different orientations.

In summary, the STM appearance of the $p(2\times2)+2$NO and $(2\times\sqrt{3})+2$NO phases on a Rh(111) surface were studied in detail both experimentally and theoretically. Since the surface system is simple and can be well characterized, we have been able to extract from STM simulations information on the structure of the different tips encountered in the experiments. We have found that blunt bcc(111) tip structures yield an excellent agreement for the entire range of experimental images after considering contamination by NO, N, or O species at different adsorption sites and appropriate tip tilts. The possibility of actively changing the tip apex in the experiment to obtain one of the simulated type of imaging enables us to choose the type of tip we want to do the experiment with. As the ignorance of the tip termination is probably the main and most long-standing drawback in STM experiments, we hope our work will open a route to more precise tip characterizations in the future.

J.C. acknowledges financial support from the Spanish MCyT under Contract No. MAT2007-66719-C03-02 and J.H. from FOM.

*c.f.j.flipse@tue.nl

[1] W. Hofer, A. Foster, and A. Shluger, Rev. Mod. Phys. **75**, 1287 (2003).
[2] J. Tersoff and D. R. Hamann, Phys. Rev. Lett. **50**, 1998 (1983).
[3] K. H. Bevan, F. Zahid, D. Kienle, and H. Guo, Phys. Rev. B **76**, 045325 (2007).
[4] J. Cerdá, M. A. Van Hove, P. Sautet, and M. Salmeron, Phys. Rev. B **56**, 15885 (1997); B. Janta-Polczynski, J. I. Cerdá, G. Ethier-Majcher, and A. Rochefort, J. Appl. Phys. (to be published); see also www.icmm.csic.es/jcerda
[5] J. Cerdá, A. Yoon, M. A. Van Hove, P. Sautet, M. Salmeron, and G. A. Somorjai, Phys. Rev. B **56**, 15900 (1997).
[6] J. M. Blanco, C. González, P. Jelinek, J. Ortega, F. Flores, and R. Perez, Phys. Rev. B **70**, 085405 (2004).
[7] Ó. Paz, I. Brihuega, J. M. Gómez-Rodríguez, and J. M. Soler, Phys. Rev. Lett. **94**, 056103 (2005).
[8] L. Bartels, G. Meyer, and K.-H. Rieder, Surf. Sci. Lett. **432**, L621 (1999).
[9] D. X. Shi, W. Ji, X. Lin, X. B. He, J. C. Lian, L. Gao, J. M. Cai, H. Lin, S. X. Du, F. Lin, C. Seidel, L. F. Chi, W. A. Hofer, H. Fuchs, and H.-J. Gao, Phys. Rev. Lett. **96**, 226101 (2006).
[10] L. Bartels, G. Meyer, and K.-H. Rieder, Appl. Phys. Lett. **71**, 213 (1997).
[11] L. Ruan, F. Besenbacher, I. Stensgaard, and E. Laegsgaard, Phys. Rev. Lett. **70**, 4079 (1993).
[12] M. Herz, F. J. Giessibl, and J. Mannhart, Phys. Rev. B **68**, 045301 (2003).
[13] F. Calleja, A. Arnau, J. J. Hinarejos, A. L. Vazquez de Parga, W. A. Hofer, P. M. Echenique, and R. Miranda, Phys. Rev. Lett. **92**, 206101 (2004).
[14] D. N. Seidman, Rev. Sci. Instrum. **78**, 30901 (2007).
[15] H. Ohnishi, Y. Kondo, and K. Takayanagi, Nature (London) **395**, 780 (1998).
[16] Y. Naitoh, K. Takayanagi, and M. Tomitori, Surf. Sci. **357–358**, 208 (1996).
[17] K. B. Rider, K. S. Hwang, M. Salmeron, and G. A. Somorjai, Phys. Rev. Lett. **86**, 4330 (2001).
[18] C. T. Kao, G. S. Blackman, M. A. Van Hove, G. A. Somorjai, and C.–M. Chan, Surf. Sci. **224**, 77 (1989).
[19] I. Zasada, M. A. van Hove, and G. A. Somorjai, Surf. Sci. **418**, L89 (1998).
[20] J. H. A. Hagelaar, Ph.D. thesis, Eindhoven University of Technology, 2008.
[21] C. J. Chen, *Introduction to Scanning Tunneling Microscopy* (Oxford University Press, New York, 1993).
[22] I. Ekvall, E. Wahlström, D. Claesson, H. Olin, and E. Olsson, Meas. Sci. Technol. **10**, 11 (1999).
[23] J. M. Soler, E. Artacho, J. Gale, A. García, J. Junquera, P. Ordejón, and D. Sánchez-Portal, J. Phys.: Condens. Matter **14**, 2745 (2002).
[24] J. P. Perdew, K. Burke, and M. Ernzerhof, Phys. Rev. Lett. **77**, 3865 (1996).
[25] J. Cerdá and F. Soria, Phys. Rev. B **61**, 7965 (2000).